

Jurassic to Neogene Quantitative Crustal Thickness Estimates in Southern Tibet

Kurt E. Sundell*, Dept. of Geosciences, University of Arizona, Tucson, Arizona 85721, USA, sundell@arizona.edu; **Andrew K. Laskowski**, Dept. of Earth Sciences, Montana State University, Bozeman, Montana 59717, USA; **Paul A. Kapp**, Dept. of Geosciences, University of Arizona, Tucson, Arizona 85721, USA; **Mihai N. Ducea**, Dept. of Geosciences, University of Arizona, Tucson, Arizona 85721, USA, and Faculty of Geology and Geophysics, University of Bucharest, 010041, Bucharest, Romania; **James B. Chapman**, Dept. of Geology and Geophysics, University of Wyoming, Laramie, Wyoming 82071, USA

ABSTRACT

Recent empirical calibrations of Sr/Y and La/Yb from intermediate igneous rocks as proxies of crustal thickness yield discrepancies when applied to high ratios from thick crust. We recalibrated Sr/Y and La/Yb as proxies of crustal thickness and applied them to the Gangdese Mountains in southern Tibet. Crustal thickness at 180–170 Ma decreased from 36 to 30 km, consistent with Jurassic backarc extension and ophiolite formation along the southern Asian margin during Neo-Tethys slab rollback. Available data preclude detailed estimates between 170 and 100 Ma and tentatively suggest ~55 km thick crust at ca. 135 Ma. Crustal thinning between 90 and 65 Ma is consistent with a phase of Neo-Tethys slab rollback that rifted a portion of the southern Gangdese arc (the Xigaze arc) from the southern Asian margin. Following the continental collision between India and Asia, crustal thickness increased by ~40 km at ~1.3 mm/a between 60 and 30 Ma to near modern crustal thickness, before the onset of Miocene east-west extension. Sustained thick crust in the Neogene suggests the onset and later acceleration of extension in southern Tibet together with ductile lower crustal flow works to balance the ongoing mass addition of under-thrusting Indian crust and maintain isostatic equilibrium.

INTRODUCTION

The Tibetan Plateau is the largest (~1,500 × 3,500 km), high-elevation (mean of ~5,000 m) topographic feature on Earth and hosts the thickest crust of any modern orogen, with estimates in southern Tibet of ~70 km (Owens and Zandt, 1997; Nábělek et al.,

2009), and up to ~85 km (Wittlinger et al., 2004; Xu et al., 2015). The Tibetan Plateau formed from the sequential accretion of continental fragments and island arc terranes beginning during the Paleozoic and culminated with the Cenozoic collision between India and Asia (Argand, 1922; Yin and Harrison, 2000; Kapp and DeCelles, 2019). The India-Asia collision is largely thought to have commenced between 60 and 50 Ma (e.g., Rowley, 1996; Hu et al., 2016); however, some raise the possibility for later collisional onset (e.g., Aitchison et al., 2007; van Hinsbergen et al., 2012). Despite ongoing ~north-south convergence, the northern Himalaya and Tibetan Plateau interior are undergoing east-west extension, expressed as an array of approximately north-trending rifts that extend from the axis of the high Himalayas to the Bangong Suture Zone (Molnar and Tapponnier, 1978; Taylor and Yin, 2009) (Fig. 1).

The Mesozoic tectonic evolution of the southern Asian margin placed critical initial conditions for the Cenozoic evolution of the Tibetan Plateau. However, much of the Mesozoic geologic history remains poorly understood, in part due to structural, magmatic, and erosional modification during the Cenozoic. There is disagreement even on first-order aspects of the Mesozoic geology in the region. For example, temporal changes in Mesozoic crustal thickness are largely unknown, and the paleoelevation of the region is debated. Most tectonic models invoke major shortening and crustal thickening due to shallow subduction during the Late Cretaceous (e.g., Wen et al., 2008; Guo et al., 2013), possibly pre-conditioning the southern Asian margin as an Andean-style

proto-plateau (Kapp et al., 2007; Lai et al., 2019). Alternatively, Late Cretaceous to Paleogene shortening may have been punctuated by a 90–70 Ma phase of extension that led to the rifting of a southern portion of the Gangdese arc and opening of a back-arc ocean basin (Kapp and DeCelles, 2019). These represent two competing end-member hypotheses for the Mesozoic tectonic evolution of southern Tibet that are testable by answering the question: Was the crust in southern Tibet thickening or thinning between 90 and 70 Ma?

Contrasting hypotheses about the Cenozoic tectonic evolution of southern Tibet are testable by quantifying changes in crustal thickness through time. In particular, the Paleocene tectonic evolution before, during, and after the collision between India and Asia was dependent on initial crustal thickness, and in part controlled the development of the modern Himalayan-Tibetan Plateau. Building on the hypothesis tests for the Late Cretaceous, if the crust of the southern Asian margin was thickened before or during the Paleocene, then this explains why the southern Lhasa Terrane was able to attain high elevations only a few million years after the onset of continental collisional orogenesis (Ding et al., 2014; Ingalls et al., 2018). However, if the Paleocene crust was thin, then we can ask the question: When did the crust attain modern or near modern thickness? Answering this question is a critical test of alternative tectonic models that suggest rapid surface uplift from relatively low elevation (and presumably thin crust) during the Miocene (e.g., Harrison et al., 1992; Molnar et al., 1993) or Pliocene (Dewey et al., 1988) as the product of mantle lithosphere removal (England and

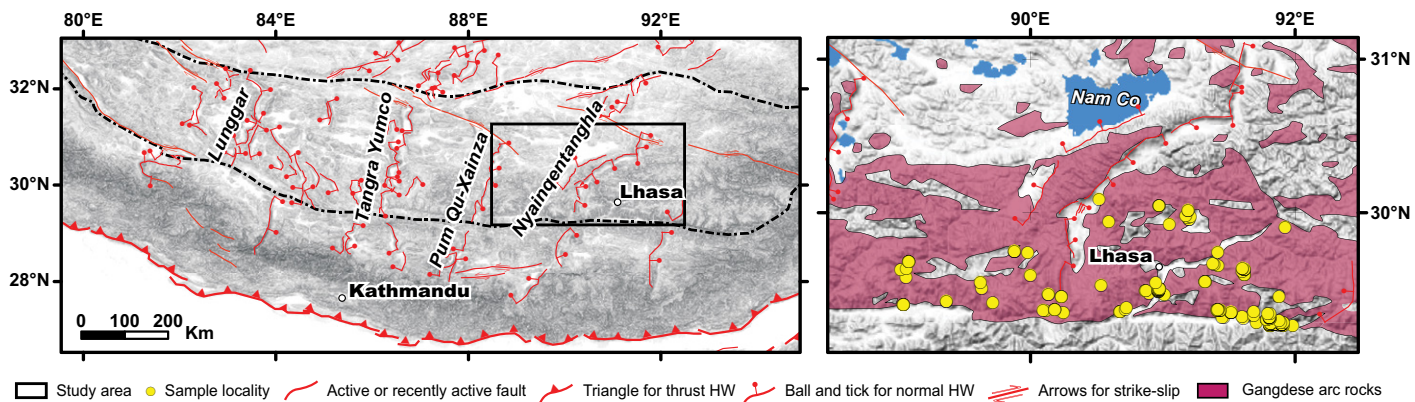


Figure 1. Digital elevation model of southern Tibet with major tectonic features. Active structures from *HimaTibetMap* (Styron et al., 2010). The basemap is from MapBox Terrain Hillshade. Lake locations are from Yan et al. (2019). Data points include only the filtered data (supplemental material [see text footnote 1]). HW—hanging wall.

Houseman, 1988). Finally, what happened after the crust was thickened to extreme levels, as we have in the modern? Did the plateau begin to undergo orogenic collapse (Dewey, 1988) resulting in a net reduction in crustal thickness and surface elevation that continues to present day (e.g., Ge et al., 2015), as evidenced by the Miocene onset of east-west extension (e.g., Harrison et al., 1995; Kapp et al., 2005; Sanchez et al., 2013; Styron et al., 2013, 2015; Sundell et al., 2013; Wolff et al., 2019)? Or did Tibet remain at steady-state elevation during Miocene-to-modern extension (Currie et al., 2005) with upper crustal thinning and ductile lower crustal flow (e.g., Royden et al., 1997) working to balance continued crustal thickening at depth driven by the northward underthrusting of India (DeCelles et al., 2002; Kapp and Guynn, 2004; Styron et al., 2015)?

Igneous rock geochemistry has long been used to estimate qualitative changes in past crustal (e.g., Heaman et al., 1990) and lithospheric (e.g., Ellam, 1992) thickness. Trace-element abundances of igneous rocks have proven particularly useful for tracking changes in crustal thickness (Kay and Mpodozis, 2002; Paterson and Ducea, 2015). Trace-element ratios provide information on the presence or absence of minerals such as garnet, plagioclase, and amphibole because their formation is pressure dependent, and each has an affinity for specific trace elements (e.g., Hildreth and Moorbath, 1988). For example, Y and Yb are preferentially incorporated into amphibole and garnet in magmatic melt residues,

whereas Sr and La have a higher affinity for plagioclase (Fig. 2A). Thus, high Sr/Y and La/Yb can be used to infer a higher abundance of garnet and amphibole and a lower abundance of plagioclase, and may be used as a proxy for assessing the depth of parent melt bodies during crustal differentiation in the lower crust (Heaman et al., 1990). These ratios have been calibrated to modern crustal thickness and paired with geochronological data to provide quantitative estimates of crustal thickness and paleoelevation through time (e.g., Chapman et al., 2015; Profeta et al., 2015; Hu et al., 2017, 2020; Farner and Lee, 2017).

We build on recent efforts to empirically calibrate trace-element ratios of igneous rocks to crustal thickness and apply these revised calibrations to the eastern Gangdese mountains in southern Tibet (Fig. 1). This region has been the focus of several studies attempting to reconstruct the crustal thickness using trace-element proxies (e.g., Zhu et al., 2017) as well as radiogenic isotopic systems such as Nd and Hf (Zhu et al., 2017; Alexander et al., 2019; DePaolo et al., 2019), and highlight discrepancies in different geochemical proxies of crustal thickness. As such, we first focus on developing a new approach to estimate crustal thickness from Sr/Y and La/Yb, both for individual ratios, and in paired Sr/Y–La/Yb calibration. We then apply these recalibrated proxies to data from the Gangdese mountains to test hypotheses explaining the Mesozoic and Cenozoic tectonic evolution of southern Tibet.

METHODS

Sr/Y and La/Yb (the latter normalized to the chondritic reservoir) were empirically calibrated using a modified approach reported in Profeta et al. (2015). Calibrations are based on simple linear regression of $\ln(\text{Sr/Y})\text{--km}$ and $\ln(\text{La/Yb})\text{--km}$; and multiple linear regression of $\ln(\text{Sr/Y})\text{--}\ln(\text{La/Yb})\text{--km}$ (Figs. 2B–2D). We also tested simple linear regression of $\ln(\text{Sr/Y}) \times \ln(\text{La/Yb})\text{--km}$ (see GSA Supplemental Material¹). Regression coefficients and residuals (known minus modeled thickness) are reported at 95% confidence ($\pm 2s$).

The revised proxies were applied to geochemical data compiled in the Tibetan Magmatism Database (Chapman and Kapp, 2017). Geochemical data used here comes from rocks collected in an area between 29 and 31°N and 89 and 92°E. Data were filtered following methods reported in Profeta et al. (2015) where samples outside compositions of 55%–68% SiO₂, 0%–4% MgO, and 0.05–0.2% Rb/Sr are excluded to avoid mantle-generated mafic rocks, high-silica felsic rocks, and rocks formed from melting of metasedimentary rocks. Filtering reduced the number of samples considered from 815 to 190 (supplemental material; see footnote 1).

We calculated temporal changes in crustal thickness based on multiple linear regression of $\ln(\text{Sr/Y})\text{--}\ln(\text{La/Yb})\text{--km}$ (Fig. 2B). Each estimate of crustal thickness is assigned uncertainty of ± 5 m.y. and ± 10 km; the former is set arbitrarily because many samples in the database do not have reported uncertainty, and the latter is based on

¹Supplemental Material. Filtered and unfiltered geochronology-geochemistry results are from the Tibetan Magmatism Database (Chapman and Kapp, 2017); the full data set between 89–92°W and 29–31°N was downloaded 20 July 2020. All data are available online at jaychapman.org/tibet-magmatism-database.html. MATLAB code is available at github.com/kurtsundell/CrustalThickness and incorporates the filtered data to reproduce all results presented in this work. Go to <https://doi.org/10.1130/GSAT.S.14271662> to access the supplemental material; contact editing@geosociety.org with any questions.

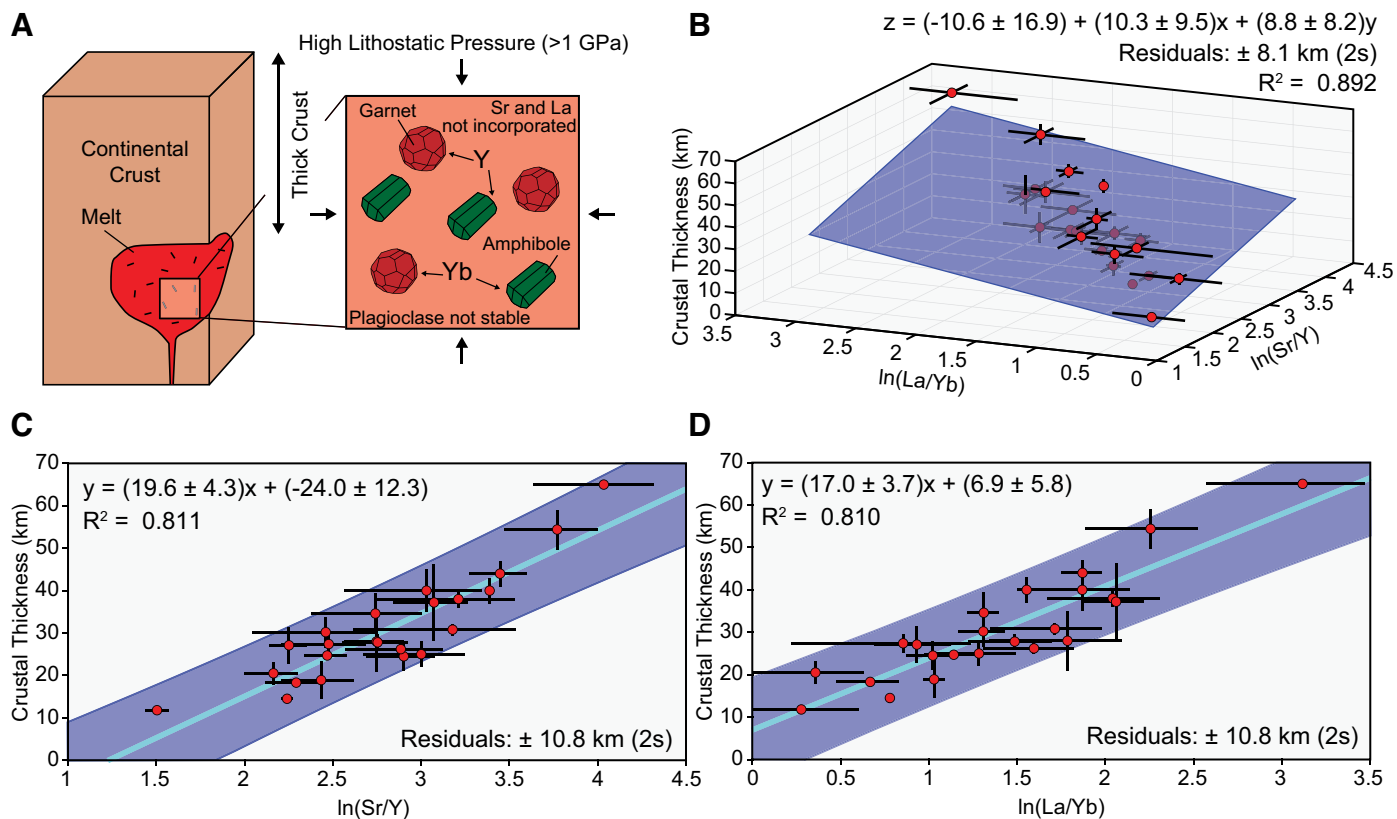


Figure 2. (A) Schematic partitioning diagram for Y and Yb into minerals stable at high lithostatic pressures >1 GPa such as garnet and amphibole. (B–D) Empirical calibrations using known crustal thicknesses from data compiled in Profeta et al. (2015) based on (B) multiple linear regression of $\ln(\text{Sr}/\text{Y})$ (x-axis), $\ln(\text{La}/\text{Yb})$ (y-axis), and crustal thickness (z-axis); (C) simple linear regression of $\ln(\text{Sr}/\text{Y})$ and crustal thickness; and (D) simple linear regression of $\ln(\text{La}/\text{Yb})$ and crustal thickness. Equations in parts B–D include 95% confidence intervals for each coefficient. Coefficient uncertainties should not be propagated when applying these equations to calculate crustal thickness; rather, the 2s (95% confidence interval) residuals (modeled fits subtracted from known crustal thicknesses) are more representative of the calibration uncertainty.

residuals calculated during proxy calibration (Fig. 2). Temporal trends were calculated using two different methods. The first method employs Gaussian kernel regression (Horová et al., 2012), a non-parametric technique commonly used to find nonlinear trends in noisy bivariate data; we used a 5 m.y. kernel width, an arbitrary parameter selected based on sensitivity testing for over- and under-smoothing. The second method involves calculating linear rates between temporal segments bracketed by clusters of data that show significant changes in crustal thickness: 200–150 Ma, 100–65 Ma, and 65–30 Ma. Trends are reported as the mean $\pm 2s$ calculated from bootstrap resampling 190 selections from the data with replacement 10,000 times.

RESULTS

Proxy calibration using simple linear regression of $\ln(\text{Sr}/\text{Y})$ –km and $\ln(\text{La}/\text{Yb})$ –km yields

$$\text{Crustal Thickness} = (19.6 \pm 4.3) \times \ln(\text{Sr}/\text{Y}) + (-24.0 \pm 12.3), \quad (1)$$

and

$$\text{Crustal Thickness} = (17.0 \pm 3.7) \times \ln(\text{La}/\text{Yb}) + (6.9 \pm 5.8), \quad (2)$$

whereas multiple linear regression of $\ln(\text{Sr}/\text{Y})$ – $\ln(\text{La}/\text{Yb})$ –km calibration yields

$$\text{Crustal Thickness} = (-10.6 \pm 16.9) + (10.3 \pm 9.5) \times \ln(\text{Sr}/\text{Y}) + (8.8 \pm 8.2) \times \ln(\text{La}/\text{Yb}). \quad (3)$$

Crustal thickness corresponds to the depth of the Moho in km, and coefficients are $\pm 2s$ (Figs. 2B–2D and supplemental material [see footnote 1]). Although we report uncertainties for the individual coefficients, propagating these uncertainties results in wildly variable (and often unrealistic) crustal thickness estimates, largely due to the highly variable slope. Hence, we ascribe uncertainties based on the 2s range of residuals (Figs. 2B–2D). Residuals are ~ 11 km based on simple linear regression of Sr/Y–km and La/Yb–km, and ~ 8 km based on multiple linear regression of Sr/Y–La/Yb–km.

Application of these equations yields mean absolute differences between crustal thicknesses calculated with individual Sr/Y and La/Yb of ~ 6 km. Paired Sr/Y–La/Yb calibration yields absolute differences of ~ 3 km compared to Sr/Y and La/Yb. Discrepancies in crustal thickness estimates between Sr/Y and La/Yb using the original calibrations in Profeta et al. (2015) are highly variable, with an average of ~ 21 km, and are largely the result of extreme crustal thickness estimates (>100 km) resulting from linear transformation of high (>70) Sr/Y ratios (supplemental material [see footnote 1]); such discrepancies are likely due to a lack of crustal thickness estimates from orogens with rocks that are young enough (i.e., Pleistocene or younger) to include in the empirical calibration.

For geologic interpretation, we use results from multiple linear regression of Sr/Y–La/Yb–km to calculate temporal changes in crustal thickness (Figs. 3B–3D). Results show a decrease in crustal thickness from 36 to 30 km between 180 and 170 Ma. Available data between 170 and 100 Ma include a single estimate of ~ 55 km at ca. 135 Ma. Crustal

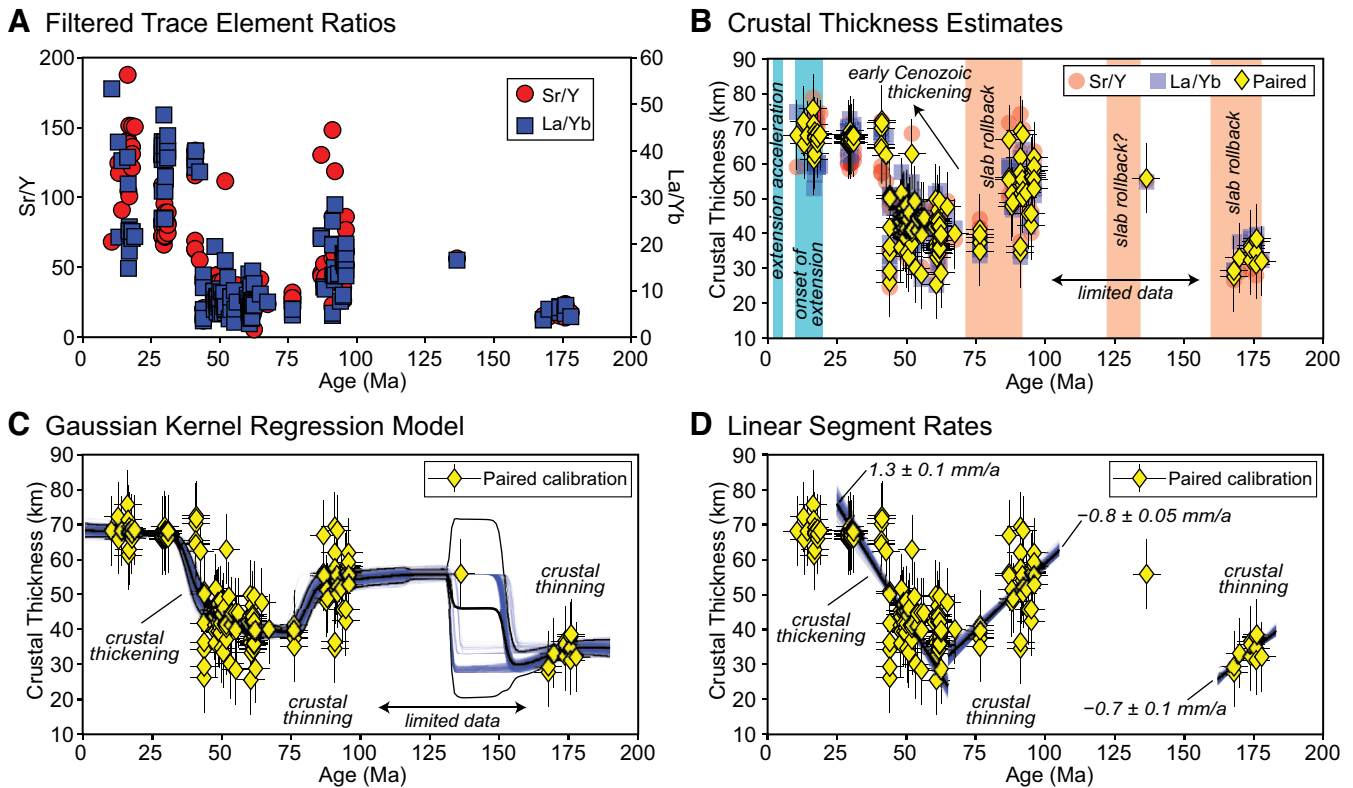


Figure 3. Results of new Sr/Y and La/Yb proxy calibration applied to data from the Tibetan Magmatism Database (Chapman and Kapp, 2017) located in the eastern Gangdese Mountains in southern Tibet. (A) Filtered Sr/Y and La/Yb data extracted from 29 to 31°N and 89 to 92°W. (B) Values from part A converted to crustal thickness using Equations 1, 2, and 3 (see text). (C–D) Temporal trends based on multiple linear regression of Sr/Y–La/Yb–km; trends are calculated from 10,000 bootstrap resamples, with replacement. (C) Gaussian kernel regression model to determine a continuous thickening history. (D) Linear regression to determine linear rates for critical time intervals.

thickness decreased to 30–50 km by ca. 60 Ma, then increased to 60–70 km by ca. 40 Ma (Fig. 3). The two different methods for calculating temporal trends in crustal thickness (Gaussian kernel regression and linear regression) produced similar results (Figs. 3C–3D). The Gaussian kernel regression model produces a smooth record of crustal thickness change that decreases from ~35 to ~30 km between 180 and 165 Ma, decreases from ~54 to ~40 km between 90 and 75 Ma, increases from ~40 to ~70 km between 60 and 40 Ma, and remains steady-state from 40 Ma to present; the large uncertainty window between 160 and 130 Ma is due to the bootstrap resampling occasionally missing the single data point at ca. 135 Ma (Fig. 3C). Linear rates of crustal thickness change indicate thinning at ~0.7 mm/a between 180 and 170 Ma, thinning at ~0.8 mm/a between 90 and 65 Ma, and thickening at ~1.3 mm/a between 60 and 30 Ma (Fig. 3D).

DISCUSSION

Early to Middle Jurassic crustal thickness in southern Tibet was controlled by the northward subduction of Neo-Tethys oceanic lithosphere (Guo et al., 2013) in an Andean

-type orogen that existed until the Early Cretaceous (Zhang et al., 2012), punctuated by backarc extension between 183 and 174 Ma (Wei et al., 2017). The latter is consistent with our results of minor crustal thinning from ~36 to ~30 km between 180 and 170 Ma (Figs. 3B–3D) and supports models invoking a period of Neo-Tethys slab rollback (i.e., trench retreat), southward rifting of the Zedong arc from the Gangdese arc, and a phase of supra-subduction zone ophiolite generation along the southern margin of Asia (Fig. 4A) (Kapp and DeCelles, 2019). Rocks with ages between 170 and 100 Ma are limited to a single data point at ca. 135 Ma and yield estimates of ~55 km thick crust (Fig. 3B–3D). This is consistent with geologic mapping and geochronological data that suggest that major north-south crustal shortening took place in the Early Cretaceous along east-west–striking thrust faults in southern Tibet (Murphy et al., 1997).

The strongest crustal thinning trend in our results occurs between 90 and 70 Ma at a rate of ~0.8 mm/a (Fig. 3D). Crustal thinning takes place after major crustal shortening (and thickening) documented in the southern Lhasa terrane prior to and up until ca. 90 Ma

(Kapp et al., 2007; Volkmer et al., 2007; Lai et al., 2019), following shallow marine carbonate deposition during the Aptian–Albian (126–100 Ma) across much of the Lhasa terrane (Leeder et al., 1988; Leier et al., 2007). Late Cretaceous crustal thinning to ~40 km (closer to the average thickness of continental crust) supports models that invoke Late Cretaceous extension and Neo-Tethys slab rollback that led to the development of an intracontinental backarc basin in southern Tibet and southward rifting of a southern portion of the Gangdese arc (referred to as the Xigaze arc) from the southern Asian continental margin (Kapp and DeCelles, 2019) (Fig. 4B). If a backarc ocean basin indeed opened between Asia and the rifted Xigaze arc during this time, it would have profound implications for Neo-Tethyan paleogeographic reconstructions and the history of suturing between India and Asia; this remains to be tested by future field-based studies.

Paleogene crustal thickness estimates indicate monotonic crustal thickening at rates of ~1.3 mm/a to >60 km following the collision between India and Asia. This is in contrast to models explaining the development of modern high elevation resulting from the removal

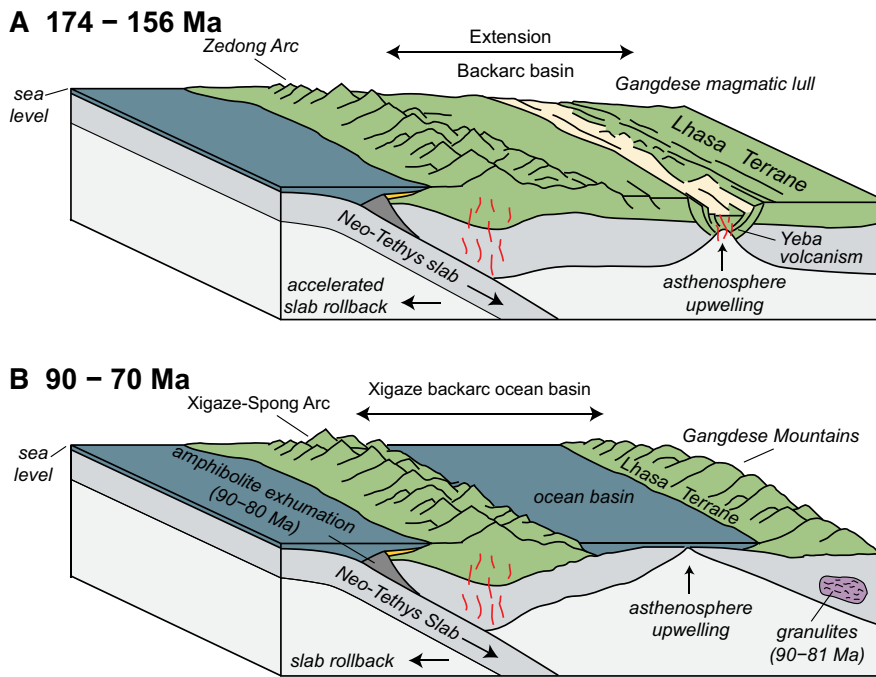


Figure 4. Tectonic interpretation after Kapp and DeCelles (2019). (A) Middle–Late Jurassic accelerated slab rollback during formation of the Zedong Arc drives the opening of an extensional backarc basin. This is consistent with the generation of the late-stage, juvenile (asthenosphere derived) Yeba volcanics (Liu et al., 2018). (B) Late Cretaceous slab rollback results in the opening of a backarc ocean basin.

of mantle lithosphere during the Miocene or Pliocene (Dewey et al., 1988; England and Houseman, 1988; Harrison et al., 1992; Molnar et al., 1993). The timing of crustal thickening in the late Paleogene temporally corresponds to the termination of arc magmatism in southern Tibet at 40–38 Ma and may indicate that the melt-fertile upper-mantle wedge was displaced to the north by shallowing subduction of Indian continental lithosphere (Laskowski et al., 2017). Crustal thickening during the Paleogene may be attributed to progressive shortening and southward propagation (with respect to India) of the Tibetan–Himalayan orogenic wedge as Indian crust was accreted in response to continuing convergence. We interpret that thickening depended mainly on the flux of crust into the orogenic wedge, as convergence between India and Asia slowed by more than 40% between 20 and 10 Ma (Molnar and Stock, 2009), subsequent to peak crustal thickening rates between 60 and 30 Ma.

Estimates of crustal thickness based on Sr/Y and La/Yb differ both in time and space compared to estimates using radiogenic isotopes. Determining crustal thickness from Nd or Hf relies on an extension of the flux-temperature model of DePaolo et al. (1992), which calculates the ambient crustal temperature and assimilation required to produce measured isotopic compositions (e.g.,

Hammersley and DePaolo, 2006) assuming a depleted asthenospheric melt source with no contribution from the mantle lithosphere; crustal thickness is then calculated based on an assumed geothermal gradient on the premise that a deeper, hotter Moho would result in more crustal assimilation than a shallower, cooler Moho. In addition to using La/Yb to estimate Cenozoic crustal thickness, DePaolo et al. (2019) use the flux-temperature model to suggest that crustal thickening in southern Tibet was nonuniform based on Nd isotopes. Specifically, they estimate crustal thickness of 25–35 km south of 29.8° N until 45 Ma, followed by major crustal thickening to 55–60 km by the early to middle Miocene. Critically, they suggest that north of 29.9° N the crust was at near modern thickness before 45 Ma and that there was a crustal discontinuity between these two domains, which Alexander et al. (2019) later interpret along orogenic strike to the east based on Hf isotopic data. In contrast, our results show that crustal thickening was already well under way by 45 Ma, potentially near modern crustal thickness, and with no dependence on latitude (Figs. 3B–3D and supplemental material [see footnote 1]). Radiogenic isotopes such as Nd and Hf are not directly controlled by crustal thickness and concomitant pressure changes. Rather, variability in Hf and Nd is likely due to complex crustal

assimilation, to which pressure-based (not temperature-based) proxies such as Sr/Y and La/Yb from rocks filtered following Profeta et al. (2015) are less sensitive.

Crustal thickness of 65–70 km between 44 and 10 Ma based on trace-element geochemistry is similar to modern crustal thickness of ~70 km estimated from geophysical methods (Owens and Zandt, 1997; Nábělek et al., 2009) and are 10–20 km less than upper estimates of 80–85 km (Wittlinger et al., 2004; Xu et al., 2015). Upper-crustal shortening persisted in southern Tibet until mid-Miocene time, but coeval rapid erosion (Copeland et al., 1995) may have maintained a uniform crustal thickness. Our results are inconsistent with models that invoke net crustal thinning via orogenic collapse (Dewey, 1988) beginning in the Miocene and continuing to present day (Ge et al., 2015). Rather, our results are consistent with interpretations of thick crust in southern Tibet by middle Eocene time (Aikman et al., 2008; Pullen et al., 2011), which continued to thicken at depth due to the ongoing mass addition of underthrusting India (DeCelles et al., 2002) before, during, and after the Miocene onset of extension in southern Tibet (e.g., Harrison et al., 1995; Kapp et al., 2005; Sanchez et al., 2013). We favor a model in which continued crustal thickening at depth is balanced by upper crustal thinning (Kapp and Guynn, 2004; DeCelles et al., 2007; Styron et al., 2015), with excess mass potentially evacuated by ductile lower crustal flow (Royden et al. 1997). In this view, late Miocene–Pliocene acceleration of rifting in southern Tibet (Styron et al., 2013; Sundell et al., 2013; Wolff et al., 2019) is a consequence of the position of the leading northern tip of India (Styron et al., 2015), because this region experiences localized thickening at depth, which in turn increases the rate of upper crustal extension in order to maintain isostatic equilibrium.

ACKNOWLEDGMENTS

We thank Chris Hawkesworth, Allen Glazner, two anonymous reviewers, and editor Peter Copeland for their detailed critique of this work. We also thank Michael Taylor and Richard Styron for informal reviews; Sarah George and Gilby Jepson for insightful discussions on proxies for crustal thickness; and Caden Howlett and Aislin Reynolds for discussions of Tibetan tectonics during the 2019 field season as this research was formulated. KES was partially supported by the National Science Foundation (EAR-1649254) at the Arizona LaserChron Center. M.N.D. acknowledges support from National Science Foundation grant EAR 1725002 and the Romanian Executive Agency for Higher Education, Research, Development and Innovation Funding project PN-III-P4-ID-PCCF-2016-0014.

REFERENCES CITED

- Aikman, A.B., Harrison, T.M., and Lin, D., 2008, Evidence for early (>44 Ma) Himalayan crustal thickening, Tethyan Himalaya, southeastern Tibet: *Earth and Planetary Science Letters*, v. 274, no. 1–2, p. 14–23, <https://doi.org/10.1016/j.epsl.2008.06.038>.
- Aitchison, J.C., Ali, J.R., and Davis, A.M., 2007, When and where did India and Asia collide?: *Journal of Geophysical Research. Solid Earth*, v. 112, no. B5, <https://doi.org/10.1029/2006JB004706>.
- Alexander, E.W., Wielicki, M.M., Harrison, T.M., DePaolo, D.J., Zhao, Z.D., and Zhu, D.C., 2019, Hf and Nd isotopic constraints on pre- and syn-collisional crustal thickness of southern Tibet: *Journal of Geophysical Research. Solid Earth*, v. 124, no. 11, p. 11,038–11,054, <https://doi.org/10.1029/2019JB017696>.
- Argand, E., 1922, June. La tectonique de l'Asie: Conférence faite à Bruxelles, le 10 août 1922.
- Chapman, J.B., and Kapp, P., 2017, Tibetan magmatism database: *Geochemistry Geophysics Geosystems*, v. 18, no. 11, p. 4229–4234, <https://doi.org/10.1002/2017GC007217>.
- Chapman, J.B., Ducea, M.N., DeCelles, P.G., and Profeta, L., 2015, Tracking changes in crustal thickness during orogenic evolution with Sr/Y: An example from the North American Cordillera: *Geology*, v. 43, no. 10, p. 919–922, <https://doi.org/10.1130/G36996.1>.
- Copeland, P., Harrison, T.M., Pan, Y., Kidd, W.S.F., Roden, M., and Zhang, Y., 1995, Thermal evolution of the Gangdese batholith, southern Tibet: A history of episodic unroofing: *Tectonics*, v. 14, no. 2, p. 223–236, <https://doi.org/10.1029/94TC01676>.
- Currie, B.S., Rowley, D.B., and Tabor, N.J., 2005, Middle Miocene paleoaltimetry of southern Tibet: Implications for the role of mantle thickening and delamination in the Himalayan orogen: *Geology*, v. 33, no. 3, p. 181–184, <https://doi.org/10.1130/G21170.1>.
- DeCelles, P.G., Robinson, D.M., and Zandt, G., 2002, Implications of shortening in the Himalayan fold-thrust belt for uplift of the Tibetan Plateau: *Tectonics*, v. 21, no. 6, p. 12-1–12-25, <https://doi.org/10.1029/2001TC001322>.
- DeCelles, P.G., Quade, J., Kapp, P., Fan, M., Dettman, D.L., and Ding, L., 2007, High and dry in central Tibet during the Late Oligocene: *Earth and Planetary Science Letters*, v. 253, no. 3–4, p. 389–401, <https://doi.org/10.1016/j.epsl.2006.11.001>.
- DePaolo, D.J., Perry, F.V., and Baldrige, W.S., 1992, Crustal versus mantle sources of granitic magmas: A two-parameter model based on Nd isotopic studies: *Transactions of the Royal Society of Edinburgh. Earth Sciences*, v. 83, no. 1–2, p. 439–446, <https://doi.org/10.1017/S0263593300008117>.
- DePaolo, D.J., Harrison, T.M., Wielicki, M., Zhao, Z., Zhu, D.C., Zhang, H., and Mo, X., 2019, Geochemical evidence for thin syn-collisional crust and major crustal thickening between 45 and 32 Ma at the southern margin of Tibet: *Gondwana Research*, v. 73, p. 123–135, <https://doi.org/10.1016/j.gr.2019.03.011>.
- Dewey, J.F., 1988, Extensional collapse of orogens: *Tectonics*, v. 7, no. 6, p. 1123–1139, <https://doi.org/10.1029/TC007i006p01123>.
- Dewey, J.F., Shackleton, R.M., Chengfa, C., and Yiyin, S., 1988, The tectonic evolution of the Tibetan Plateau: *Philosophical Transactions of the Royal Society of London. Series A, Mathematical and Physical Sciences*, v. 327, no. 1594, p. 379–413.
- Ding, L., Xu, Q., Yue, Y., Wang, H., Cai, F., and Li, S., 2014, The Andean-type Gangdese Mountains: Paleolevation record from the Paleocene–Eocene Linzhou Basin: *Earth and Planetary Science Letters*, v. 392, p. 250–264, <https://doi.org/10.1016/j.epsl.2014.01.045>.
- Ellam, R.M., 1992, Lithospheric thickness as a control on basalt geochemistry: *Geology*, v. 20, no. 2, p. 153–156, [https://doi.org/10.1130/0091-7613\(1992\)020<0153:LTAACO>2.3.CO;2](https://doi.org/10.1130/0091-7613(1992)020<0153:LTAACO>2.3.CO;2).
- England, P.C., and Houseman, G.A., 1988, The mechanics of the Tibetan Plateau: *Philosophical Transactions of the Royal Society of London. Series A, Mathematical and Physical Sciences*, v. 326, no. 1589, p. 301–320.
- Farner, M.J., and Lee, C.T.A., 2017, Effects of crustal thickness on magmatic differentiation in subduction zone volcanism: A global study: *Earth and Planetary Science Letters*, v. 470, p. 96–107, <https://doi.org/10.1016/j.epsl.2017.04.025>.
- Ge, W.P., Molnar, P., Shen, Z.K., and Li, Q., 2015, Present-day crustal thinning in the southern and northern Tibetan plateau revealed by GPS measurements: *Geophysical Research Letters*, v. 42, no. 13, p. 5227–5235, <https://doi.org/10.1002/2015GL064347>.
- Guo, L., Liu, Y., Liu, S., Cawood, P.A., Wang, Z., and Liu, H., 2013, Petrogenesis of Early to Middle Jurassic granitoid rocks from the Gangdese belt, Southern Tibet: Implications for early history of the Neo-Tethys: *Lithos*, v. 179, p. 320–333, <https://doi.org/10.1016/j.lithos.2013.06.011>.
- Hammersley, L., and DePaolo, D.J., 2006, Isotopic and geophysical constraints on the structure and evolution of the Clear Lake volcanic system: *Journal of Volcanology and Geothermal Research*, v. 153, no. 3–4, p. 331–356, <https://doi.org/10.1016/j.jvolgeores.2005.12.003>.
- Harrison, T.M., Copeland, P., Kidd, W.S.F., and Lovera, O.M., 1995, Activation of the Nyainqentanghla shear zone: Implications for uplift of the southern Tibetan Plateau: *Tectonics*, v. 14, no. 3, p. 658–676, <https://doi.org/10.1029/95TC00608>.
- Heaman, L.M., Bowins, R., and Crocket, J., 1990, The chemical composition of igneous zircon suites: Implications for geochemical tracer studies: *Geochimica et Cosmochimica Acta*, v. 54, no. 6, p. 1597–1607, [https://doi.org/10.1016/0016-7037\(90\)90394-Z](https://doi.org/10.1016/0016-7037(90)90394-Z).
- Hildreth, W., and Moorbath, S., 1988, Crustal contributions to arc magmatism in the Andes of central Chile: Contributions to Mineralogy and Petrology, v. 98, no. 4, p. 455–489, <https://doi.org/10.1007/BF00372365>.
- Horová, I., Koláček, J., and Zelinka, J., 2012, Kernel smoothing in MATLAB: Theory and practice of kernel smoothing: *Toh Tuck Link*, Singapore, World Scientific Publishing Co. Pte. Ltd., p. 137–178.
- Hu, F., Ducea, M.N., Liu, S., and Chapman, J.B., 2017, Quantifying crustal thickness in continental collisional belts: Global perspective and a geologic application: *Scientific Reports*, v. 7, no. 1, 7058, p. 1–10, <https://doi.org/10.1038/s41598-017-07849-7>.
- Hu, F., Wu, F., Chapman, J.B., Ducea, M.N., Ji, W., and Liu, S., 2020, Quantitatively tracking the elevation of the Tibetan Plateau since the Cretaceous: Insights from whole-rock Sr/Y and La/Yb ratios: *Geophysical Research Letters*, v. 47, no. 15, <https://doi.org/10.1029/2020GL089202>.
- Hu, X., Wang, J., BouDagher-Fadel, M., Garzanti, E., and An, W., 2016, New insights into the timing of the India–Asia collision from the Paleogene Quxia and Jialazi formations of the Xigaze forearc basin, South Tibet: *Gondwana Research*, v. 32, p. 76–92, <https://doi.org/10.1016/j.gr.2015.02.007>.
- Ingalls, M., Rowley, D., Olack, G., Currie, B., Li, S., Schmidt, J., Tremblay, M., Polissar, P., Shuster, D.L., Lin, D., and Colman, A., 2018, Paleocene to Pliocene low-latitude, high-elevation basins of southern Tibet: Implications for tectonic models of India-Asia collision, Cenozoic climate, and geochemical weathering: *Geological Society of America Bulletin*, v. 130, no. 1–2, p. 307–330, <https://doi.org/10.1130/B31723.1>.
- Kapp, J.L.D., Harrison, T.M., Kapp, P., Grove, M., Lovera, O.M., and Lin, D., 2005, Nyainqentanghla Shan: A window into the tectonic, thermal, and geochemical evolution of the Lhasa block, southern Tibet: *Journal of Geophysical Research. Solid Earth*, v. 110, B8, <https://doi.org/10.1029/2004JB003330>.
- Kapp, P., and DeCelles, P.G., 2019, Mesozoic–Cenozoic geological evolution of the Himalayan–Tibetan orogen and working tectonic hypotheses: *American Journal of Science*, v. 319, no. 3, p. 159–254, <https://doi.org/10.2475/03.2019.01>.
- Kapp, P., and Guynn, J.H., 2004, Indian punch rifts Tibet: *Geology*, v. 32, no. 11, p. 993–996, <https://doi.org/10.1130/G20689.1>.
- Kapp, P., DeCelles, P.G., Gehrels, G.E., Heizler, M., and Ding, L., 2007, Geological records of the Lhasa–Qiangtang and Indo–Asian collisions in the Nima area of central Tibet: *Geological Society of America Bulletin*, v. 119, no. 7–8, p. 917–933, <https://doi.org/10.1130/B26033.1>.
- Kay, S.M., and Mpodozis, C., 2002, Magmatism as a probe to the Neogene shallowing of the Nazca plate beneath the modern Chilean flat-slab: *Journal of South American Earth Sciences*, v. 15, no. 1, p. 39–57, [https://doi.org/10.1016/S0895-9811\(02\)00005-6](https://doi.org/10.1016/S0895-9811(02)00005-6).
- Lai, W., Hu, X., Garzanti, E., Sun, G., Garzzone, C.N., Fadel, M.B., and Ma, A., 2019, Initial growth of the Northern Lhasaplano, Tibetan Plateau in the early Late Cretaceous (ca. 92 Ma): *Geological Society of America Bulletin*, v. 131, no. 11–12, p. 1823–1836, <https://doi.org/10.1130/B35124.1>.
- Laskowski, A.K., Kapp, P., Ding, L., Campbell, C., and Liu, X., 2017, Tectonic evolution of the Yarlung suture zone, Lopu Range region, southern Tibet: *Tectonics*, v. 36, no. 1, p. 108–136, <https://doi.org/10.1002/2016TC004334>.
- Leeder, M.R., Smith, A.B., and Jixiang, Y., 1988, Sedimentology, palaeoecology and palaeoenvironmental evolution of the 1985 Lhasa to Golmud Geotraverse: *Philosophical Transactions of the Royal Society of London, Series A, Mathematical and Physical Sciences*, v. 327, no. 1594, p. 107–143.
- Leier, A.L., Kapp, P., Gehrels, G.E., and DeCelles, P.G., 2007, Detrital zircon geochronology of Carboniferous–Cretaceous strata in the Lhasa terrane, Southern Tibet: *Basin Research*, v. 19, no. 3, p. 361–378, <https://doi.org/10.1111/j.1365-2117.2007.00330.x>.
- Liu, Z.C., Ding, L., Zhang, L.Y., Wang, C., Qiu, Z.L., Wang, J.G., Shen, X.L., and Deng, X.Q., 2018,

- Sequence and petrogenesis of the Jurassic volcanic rocks (Yeba Formation) in the Gangdese arc, southern Tibet: Implications for the Neo-Tethyan subduction: *Lithos*, v. 312–313, p. 72–88, <https://doi.org/10.1016/j.lithos.2018.04.026>.
- Molnar, P., and Stock, J.M., 2009, Slowing of India's convergence with Eurasia since 20 Ma and its implications for Tibetan mantle dynamics: *Tectonics*, v. 28, no. 3, <https://doi.org/10.1029/2008TC002271>.
- Molnar, P., and Tapponnier, P., 1978, Active tectonics of Tibet: *Journal of Geophysical Research. Solid Earth*, v. 83, B11, p. 5361–5375, <https://doi.org/10.1029/JB083iB11p05361>.
- Molnar, P., England, P., and Martinod, J., 1993, Mantle dynamics, uplift of the Tibetan Plateau, and the Indian monsoon: *Reviews of Geophysics*, v. 31, no. 4, p. 357–396, <https://doi.org/10.1029/93RG02030>.
- Murphy, M.A., Yin, A., Harrison, T.M., Durr, S.B., Ryerson, F.J., and Kidd, W.S.F., 1997, Did the Indo-Asian collision alone create the Tibetan plateau?: *Geology*, v. 25, no. 8, p. 719–722, [https://doi.org/10.1130/0091-7613\(1997\)025<0719:DTIACA>2.3.CO;2](https://doi.org/10.1130/0091-7613(1997)025<0719:DTIACA>2.3.CO;2).
- Nábělek, J., Hetényi, G., Vergne, J., Sapkota, S., Kafle, B., Jiang, M., Su, H., Chen, J., and Huang, B.S., 2009, Underplating in the Himalaya-Tibet collision zone revealed by the Hi-CLIMB experiment: *Science*, v. 325, no. 5946, p. 1371–1374, <https://doi.org/10.1126/science.1167719>.
- Owens, T.J., and Zandt, G., 1997, Implications of crustal property variations for models of Tibetan plateau evolution: *Nature*, v. 387, no. 6628, p. 37–43, <https://doi.org/10.1038/387037a0>.
- Paterson, S.R., and Ducea, M.N., 2015, Arc magmatic tempos: Gathering the evidence: *Elements*, v. 11, no. 2, p. 91–98, <https://doi.org/10.2113/gselements.11.2.91>.
- Profeta, L., Ducea, M.N., Chapman, J.B., Paterson, S.R., Gonzales, S.M.H., Kirsch, M., Petrescu, L., and DeCelles, P.G., 2015, Quantifying crustal thickness over time in magmatic arcs: *Scientific Reports*, v. 5, 17786, <https://doi.org/10.1038/srep17786>.
- Pullen, A., Kapp, P., Gehrels, G.E., Ding, L., and Zhang, Q., 2011, Metamorphic rocks in central Tibet: Lateral variations and implications for crustal structure: *Geological Society of America Bulletin*, v. 123, no. 3–4, p. 585–600, <https://doi.org/10.1130/B30154.1>.
- Rowley, D.B., 1996, Age of initiation of collision between India and Asia: A review of stratigraphic data: *Earth and Planetary Science Letters*, v. 145, no. 1–4, p. 1–13, [https://doi.org/10.1016/S0012-821X\(96\)00201-4](https://doi.org/10.1016/S0012-821X(96)00201-4).
- Royden, L.H., Burchfiel, B.C., King, R.W., Wang, E., Chen, Z., Shen, F., and Liu, Y., 1997, Surface deformation and lower crustal flow in eastern Tibet: *Science*, v. 276, 5313, p. 788–790, <https://doi.org/10.1126/science.276.5313.788>.
- Sanchez, V.I., Murphy, M.A., Robinson, A.C., Lapen, T.J., and Heizler, M.T., 2013, Tectonic evolution of the India–Asia suture zone since Middle Eocene time, Lopukangri area, south-central Tibet: *Journal of Asian Earth Sciences*, v. 62, p. 205–220, <https://doi.org/10.1016/j.jseas.2012.09.004>.
- Styron, R., Taylor, M., and Okoronkwo, K., 2010, Database of active structures from the Indo-Asian collision: *Eos*, v. 91, no. 20, p. 181–182, <https://doi.org/10.1029/2010EO200001>.
- Styron, R.H., Taylor, M.H., Sundell, K.E., Stockli, D.F., Oalman, J.A., Möller, A., McCallister, A.T., Liu, D., and Ding, L., 2013, Miocene initiation and acceleration of extension in the South Lunggar rift, western Tibet: Evolution of an active detachment system from structural mapping and (U-Th)/He thermochronology: *Tectonics*, v. 32, no. 4, p. 880–907, <https://doi.org/10.1002/tect.20053>.
- Styron, R., Taylor, M., and Sundell, K., 2015, Accelerated extension of Tibet linked to the northward underthrusting of Indian crust: *Nature Geoscience*, v. 8, no. 2, p. 131–134, <https://doi.org/10.1038/ngeo2336>.
- Sundell, K.E., Taylor, M.H., Styron, R.H., Stockli, D.F., Kapp, P., Hager, C., Liu, D., and Ding, L., 2013, Evidence for constriction and Pliocene acceleration of east-west extension in the North Lunggar rift region of west central Tibet: *Tectonics*, v. 32, no. 5, p. 1454–1479, <https://doi.org/10.1002/tect.20086>.
- Taylor, M., and Yin, A., 2009, Active structures of the Himalayan-Tibetan orogen and their relationships to earthquake distribution, contemporary strain field, and Cenozoic volcanism: *Geosphere*, v. 5, no. 3, p. 199–214, <https://doi.org/10.1130/GES00217.1>.
- van Hinsbergen, D.J., Lippert, P.C., Dupont-Nivet, G., McQuarrie, N., Doubrovine, P.V., Spakman, W., and Torsvik, T.H., 2012, Greater India Basin hypothesis and a two-stage Cenozoic collision between India and Asia: *Proceedings of the National Academy of Sciences of the United States of America*, v. 109, no. 20, p. 7659–7664, <https://doi.org/10.1073/pnas.1117262109>.
- Volkmer, J.E., Kapp, P., Guynn, J.H., and Lai, Q., 2007, Cretaceous–Tertiary structural evolution of the north central Lhasa terrane, Tibet: *Tectonics*, v. 26, no. 6, <https://doi.org/10.1029/2005TC001832>.
- Wei, Y., Zhao, Z., Niu, Y., Zhu, D.C., Liu, D., Wang, Q., Hou, Z., Mo, X., and Wei, J., 2017, Geochronology and geochemistry of the Early Jurassic Yeba Formation volcanic rocks in southern Tibet: Initiation of back-arc rifting and crustal accretion in the southern Lhasa Terrane: *Lithos*, v. 278–281, p. 477–490, <https://doi.org/10.1016/j.lithos.2017.02.013>.
- Wen, D.R., Liu, D., Chung, S.L., Chu, M.F., Ji, J., Zhang, Q., Song, B., Lee, T.Y., Yeh, M.W., and Lo, C.H., 2008, Zircon SHRIMP U-Pb ages of the Gangdese Batholith and implications for Neotethyan subduction in southern Tibet: *Chemical Geology*, v. 252, no. 3–4, p. 191–201, <https://doi.org/10.1016/j.chemgeo.2008.03.003>.
- Wittlinger, G., Vergne, J., Tapponnier, P., Farra, V., Poupinet, G., Jiang, M., Su, H., Herquel, G., and Paul, A., 2004, Teleseismic imaging of subducting lithosphere and Moho offsets beneath western Tibet: *Earth and Planetary Science Letters*, v. 221, no. 1–4, p. 117–130, [https://doi.org/10.1016/S0012-821X\(03\)00723-4](https://doi.org/10.1016/S0012-821X(03)00723-4).
- Wolff, R., Hetzel, R., Dunkl, I., Xu, Q., Bröcker, M., and Anczkiewicz, A.A., 2019, High-angle normal faulting at the Tangra Yumco Graben (Southern Tibet) since ~15 Ma: *The Journal of Geology*, v. 127, no. 1, p. 15–36, <https://doi.org/10.1086/700406>.
- Xu, Q., Zhao, J., Yuan, X., Liu, H., and Pei, S., 2015, Mapping crustal structure beneath southern Tibet: Seismic evidence for continental crustal underthrusting: *Gondwana Research*, v. 27, no. 4, p. 1487–1493, <https://doi.org/10.1016/j.gr.2014.01.006>.
- Yan, D., Li, M., Bi, W., Weng, B., Qin, T., Wang, J., and Do, P., 2019, A data set of inland lake catchment boundaries for the Qiangtang Plateau: *Scientific Data*, v. 6, no. 1, p. 1–11.
- Yin, A., and Harrison, T.M., 2000, Geologic evolution of the Himalayan-Tibetan orogen: *Annual Review of Earth and Planetary Sciences*, v. 28, no. 1, p. 211–280, <https://doi.org/10.1146/annurev.earth.28.1.211>.
- Zhang, K.J., Zhang, Y.X., Tang, X.C., and Xia, B., 2012, Late Mesozoic tectonic evolution and growth of the Tibetan plateau prior to the Indo-Asian collision: *Earth-Science Reviews*, v. 114, no. 3–4, p. 236–249, <https://doi.org/10.1016/j.earscirev.2012.06.001>.
- Zhu, D.C., Wang, Q., Cawood, P.A., Zhao, Z.D., and Mo, X.X., 2017, Raising the Gangdese mountains in southern Tibet: *Journal of Geophysical Research. Solid Earth*, v. 122, no. 1, p. 214–223, <https://doi.org/10.1002/2016JB013508>.

MANUSCRIPT RECEIVED 16 APR. 2020

REVISION RECEIVED 1 SEPT. 2020

MANUSCRIPT ACCEPTED 8 MAR. 2021